Perovskite $BaCrO_3$: completing a materials system with an anomalous Mott transition

Z. H. Zhu,[1] F. J. Rueckert[1], J. I. Budnick,[1,2] W. A. Hines,[1] M. Jain,[1,2] H. Zhang,[2] and B. O. Wells[1]
[1]Department of Physics, University of Connecticut, Storrs, Connecticut 06269-3046
[2]Institute of Material Science, University of Connecticut, Storrs, Connecticut 06269-3136, USA
(Dated: November 5, 2012)

We have synthesized and characterized laser-deposited film samples of perovskite $BaCrO_3$, a missing member of the perovskite-chromate family. The $BaCrO_3$ films have a substantially larger lattice constant than other chromates, are insulating, and exhibit weak ferromagnetism likely associated with canted antiferromagnetism. Comparison with the other sister compounds $CaCrO_3$ and $SrCrO_3$ suggest an anomalous Mott transition where magnetism is independent of whether the compound is metallic or insulating

Transition metal oxides (TMOs) with perovskite and related structures exhibit many fascinating electronic phenomena, including Mott insulators, metal-insulator transitions, and high-Tc superconductivity, due to transport being determined by strongly correlated d electrons.[1] One of the key ubiquitous questions for these compounds is how exactly transport is coupled to magnetic degrees of freedom. The textbook situation is that ferromagnetism leads to metallic conductivity, while antiferromagnetism is associated with non-conducting behavior, particularly Mott insulators. A classic example is colossal magnetoresistance in the manganites, where a magnetic field can induce a transition from an insulating antiferromagnetic phase to a conducting, ferromagnetic phase.[2] There are some exceptions which indicate other new phenomena may be in play. Observations of ferromagnetic insulators and antiferromagnetic conductors are most often explained by particular orbital orderings[3] or reduced electronic and structural dimensionality.[4] This report describes the properties of a new end member of a system that can be driven through a metal-insulator transition using chemical pressure, or bandwidth control, yet seems to retain the same magnetic structure on both sides of the transition. We have synthesized $BaCrO_3$ in perovskite form. This polymorph is apparently not stable in the bulk, and only stabilized using epitaxial film growth on an appropriate crystal template.

Four decades ago, a few chromate perovskites $ACrO_3$ (A = Ca, Sr, and Pb) were synthesized by several groups using solid-state reaction techniques with high pressure ($\approx$ 6-10 GPa) and high temperature ($\approx$ 1000 K).[5−9] Recent studies on $CaCrO_3$ and $SrCrO_3$ have produced controversial results, drawing more attention to these chromate compounds.[10−16] $CaCrO_3$, with the orthorhombic structure, was reported to be metallic with an antiferromagnetic (AFM) spin structure.[8] However, J. -S. Zhou et al.10 reported that $CaCrO_3$ is an insulator and that the metallic phase only exists under high pressure. Some recent studies done by A. C. Kormarek et al.,[13] concluded that $CaCrO_3$ is metallic and antiferromagnetic. It is also suggested that $CaCrO_3$ possibly lies in the crossover region between being itinerant and localized, implying the necessity to consider correlation effects.[14,15] A similar issue is also debated in the case of $SrCrO_3$, which was reported to be metallic-like along with Pauli paramagnetic behavior in an early study,[6] but the metallic phase was observed recently only under high pressure.[10] In addition to its controversial electronic transport properties, an interesting orbital ordering transition and electronic phase coexistence have been discovered in $SrCrO_3$.[12]

Among these chromate compounds, only $PbCrO_3$ is unambiguously thought to be an insulator with the G-type AFM spin structure. However, because of the different outer orbital configuration of Pb, $PbCrO_3$ can hardly be used to form a unified scheme to understand the controversial properties of the other chromate family compounds. On the other hand, perovskite $BaCrO_3$, which should be akin to $CaCrO_3$ and $SrCrO_3$, has not been formed as yet using traditional solid-state reaction methods. It seems that $BaCrO_3$ tends to form a hexagonal phase.[17,18] This can be understood by considering the tolerance factor $t = (r_A+r_O)/\sqrt{2}(r_B+r_O)$, where r_A, r_B, and r_O are the ionic radii of the A, B cations, and oxygen anion, respectively.[19] Typically, perovskite structures have $t < 1$, while hexagonal polytypes result when $t > 1$. The tolerance factor of $BaCrO_3$ is 1.031, which is slightly above the allowed range for a cubic perovskite phase. Epitaxial film growth on an appropriate substrate has been known as a method for stabilizing particular phases. Here we have successfully used well lattice-matched $SrTO_3$(STO) (001) surfaces as a template for growing perovskite $BaCrO_3$ using pulsed laser deposition (PLD) and are able to measure its basic properties.

The laser target was a stoichiometric mixture of BaO and Cr_2O_3 prepared by solid-state reaction at 1000^{oC} in air. During growth, the substrate temperature was kept at 800 ^{oC} in 10^{-7} torr vacuum. After deposition, the films were cooled to room temperature at a rate of 4^{oC} per minute. The film growth was found to be extremely sensitive to both the vacuum conditions and temperature of the substrate. Growing the film in oxygen atmosphere always resulted in $BaCrO_4$.

The crystal structure of the $BaCrO_3$ film was determined using both a two-circle x-ray diffractometer to study peaks perpendicular to the surface and a three-circle diffractometer with an area detector for determining in- and out-of-plane lattice constants. All of the x-ray

data used Cu Kα ($\lambda = 1.540598$Å) radiation. X-ray photoemission spectroscopy (XPS) was performed in order to study the composition and purity of the $BaCrO_3$ film using a PHI Multiprobe with Al anode. Measurements of the dc magnetization were made on a Quantum Design MPMS SQUID magnetometer for temperatures 5.0 K $\leq$ T$\leq$ 300 K and magnetic fields -50 kOe $\leq$ H $\leq$ +50 kOe. Finally, resistivity measurements were carried out using a conventional four-probe technique along with the variable temperature and magnetic field control of the MPMS.

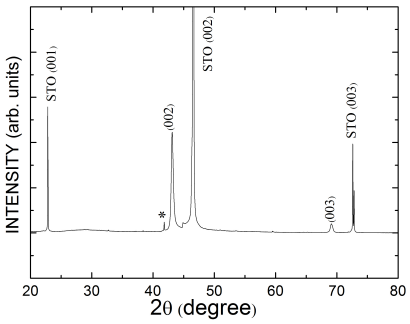

FIG. 1: X-ray diffraction pattern for a typical epitaxial BaCrO3 thin film on a STO(001) substrate. The (002) and (003) $BaCrO_3$ film peaks, which occur at 43.12^o and 69.09^o, respectively, identify the "cubic " perovskite . The small peak labeled with (*) at 41.82^o corresponds to the STO substrate (002) Kβ reflection. The small step-like feature at 44.90^o is an experimental artifact related to the window size of the detector.

Figure 1 shows the x-ray diffraction(XRD) pattern for out-of-plane peaks of a typical epitaxial $BaCrO_3$ film on a STO(001) substrate. The $BaCrO_3$ film peaks at 43.12^o and 69.09^o correspond to the (002) and (003) reflections, respectively, and identify the "cubic"perovskite structure. This result is unlike the case for powders where the hexagonal structure has been observed.[17,18] The lattice constants are measured on an oxford single crystal diffractometer and give the following room-temperature values: out-of-plane lattice constant c = 4.07Å, in-plane lattice constant a = 4.09Å. In comparison, the pseudocubic lattice parameter for bulk $CaCrO_3$ and $SrCrO_3$ are 3.75Åand 3.82Å, respectively. The trend is that as the atomic number increases from Ca (20) to Ba (58), the lattice constant increases significantly. The structure of our film samples thus has a small tetragonal distortion from the cubic case. Tilting patterns in the BO_6 octahedra are common in perovskites, although in this case the associated superlattice peaks appear to be too weak to be detected on our film samples.

X-ray photoemission spectroscopy (XPS) was performed in order to study the chemical composition and phase purity of the film, along with the ionic state of Cr. No extra peaks due to impurities were observed except for that of Au, which is used for calibration and grounding of the film. The ratio between the Ba and Cr is found

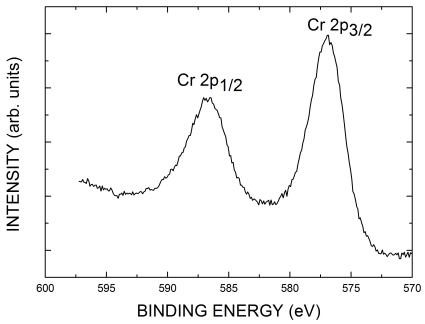

FIG. 2: High-resolution x-ray photoemission spectrum for a typical epitaxial $BaCrO^3$ thin film on a STO(001) substrate. The binding energy for the Cr core level $2p^3/2$ and $2p^1/2$ peaks are 577.1 eV and 586.8 eV, respectively, consistent with the Cr^{4+} valence state for the $BaCrO_3$ film.

to be 1:1 and remains constant throughout the thickness of the film, which was revealed by collecting spectra as we sputtered through the film. A scan of the Cr 2p core level region is shown in Fig. 2. The binding energy for the $2p^{3/2}$ and $2p^{1/2}$ peaks of Cr are 577.1 eV and 586.8 eV, respectively, which matches binding energies of main peaks due to spin-orbit splitting for $CaCrO_3$, indicating the Cr^{4+} valence state in the $BaCrO_3$ films.[16] Our spectrum in Fig. 2 overall is very similar to that for $CaCrO_3$ in Ref. 16, though we appear to have slightly poorer resolution which does not allow us to detect additional shoulder-like features reported in the latter

The $BaCrO_3$ films have a small, but definite magnetic response. Measurement of this signal is complicated by the small size of the film signal compared to the relatively large contribution of the substrate. Magnetic measurements were carried out for the magnetic field aligned both parallel and perpendicular to the film/substrate. For the parallel case, the samples were mounted onto a uniform quartz rod with a very small amount of two-sided tape. For the perpendicular case, the samples were inside a small diameter plastic straw, held in place by cotton. The magnetic characteristics of a blank STO(001) substrate were measured with both orientations for temperatures 5 K $\leq$ T $\leq$ 300 K and magnetic fields -50 kOe $\leq$ H $\leq$ +50 kOe. In addition to the diamagnetic response of the STO substrate material, other background effects were present. These included: (1) trace amounts of magnetic impurities in the STO substrate material, (2) magnetic response of the cotton, which was predominately diamagnetic, and (3) trace amounts of oxygen in the SQUID sample chamber. The presence of oxygen, which can be significantly reduced but not always completely eliminated, frequently complicates low temperature magnetic measurements. Nevertheless, the various background effects were accounted for in order to isolate the magnetic response of the $BaCrO_3$ film. Figure 3 shows the zero-field-cooled (ZFC) and field-cooled (FC) curves obtained for a magnetic field H = 500 Oe (H parallel) from a typical $BaCrO_3$ film on a STO(001)

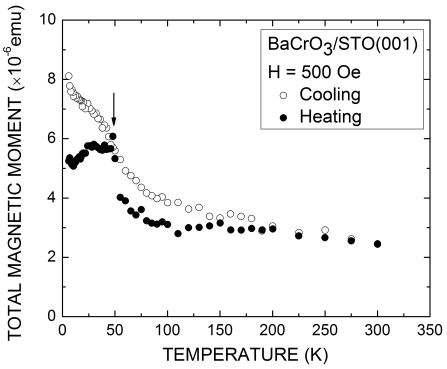

FIG. 3: Zero-field-cooled (ZFC) and field-cooled (FC) dc magnetization versus temperature for a magnetic field H = 500 Oe (H parallel) from a typical epitaxial $BaCrO_3$ thin film on a STO(001) substrate: closed circles - heating, open circles - cooling). There is a peak in the ZFC curve at T ≈ 25 K, below which the ZFC and FC curves significantly bifurcate, suggesting the onset of magnetic ordering. The offset (≈3 × 10^{-6} emu) is due to magnetic impurities in the substrate material while the small feature at ≈ 48 K(arrow) is due to oxygen.

substrate. It can be seen that there is a peak in the ZFC curve at T ≈25 K, below which the ZFC and FC curves bifurcate. As discussed below, this behavior was always reproducible and is attributed to a magnetic transition associated with the $BaCrO_3$ film. In Fig. 3, the non-zero high temperature signal (≈3 × 10^{-6} emu) is primarily due to magnetic impurities in the substrate.

In order to explore the nature of the magnetic ordering for the $BaCrO_3$ film on a STO(001) substrate, full hysteresis loops (-50 kOe ≤ H ≤ +50 kOe) were obtained for temperatures above and below the T ≈25 K transition, principally for T = 300 K, 150 K, and 10 K. All of the loops obtained show a dominant diamagnetic contribution due to the STO(001) substrate along with a much smaller ferromagnetic contribution. As an example, Fig. 4a shows the total as-measured hysteresis loop magnetization obtained at 10 K from a sample consisting of a typical $BaCrO_3$ film on a STO(001) substrate with H parallel to the film/substrate. Figure 4b shows the hysteresis loop magnetization in Fig. 4a with the diamagnetic part of the substrate contribution subtracted off. The resulting curve in Fig. 4b is characteristic of weak ferromagnetic behavior with a small coercive field and a magnetization that saturates for H ≥ 1,000 Oe. Figure 4c shows the values of the saturation magnetic moment, for T = 10 K, 150 K, and 300 K, obtained from curves such as shown in Fig. 4b. The closed (open) symbols represent values obtained for H parallel (perpendicular) to the film/substrate. The saturation magnetic moment values obtained for T = 150 K and 300 K (above the 25 K transition temperature) are the background contributions from the substrate and cotton. Similar measurements on blank substrates revealed that the background

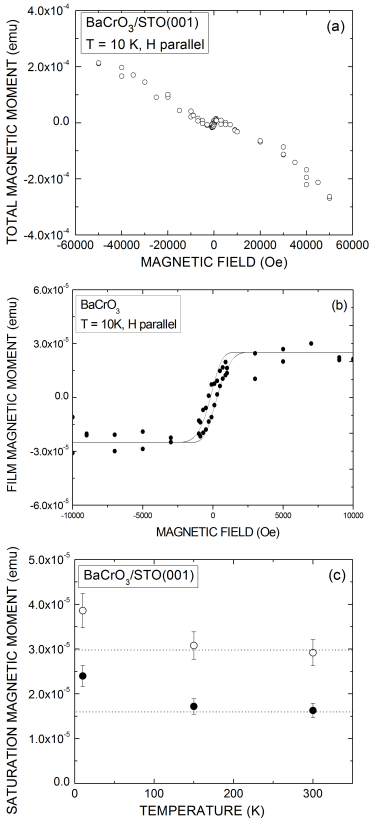

FIG. 4: (a) Hysteresis loop magnetization at 10 K for a typical $BaCrO_3$ thin film on a STO(001) substrate with H parallel to the film/substrate. The negative slope reflects the dominant diamagnetic response for the STO(001) substrate. (b) Hysteresis loop magnetization from (a) corrected for the diamagnetic contribution of the substrate. The resulting curve is characteristic of weak ferromagnetic behavior with a small coercive field and a magnetization that saturates for H âĽě 1,000 Oe. The solid line is a guide to the eye. (c) Saturation magnetic moment values versus temperature obtained from curves such as shown in (b). The closed (open) symbols represent values obtained for H parallel (perpendicular) to the film/substrate. The moment values obtained for T = 150 K and 300 K (above the 25 K transition temperature) are the background contributions from the substrate and cotton, while the larger moment values obtained at T = 10 K include the contribution from the $BaCrO_3$ film.

contributions were essentially temperature independent. On the other hand, the saturation magnetization values obtained at T = 10 K (below the 25 K transition temperature) shown in Fig. 4c include a contribution from the $BaCrO_3$ film. This behavior was reproducible in other film/substrate samples. Thus, the saturation moment for epitaxial $BaCrO_3$ film can be obtained by subtraction. Taking the saturation magnetic moment value of 0.7 × 10^{-5} emu (see Fig. 4c), with a film thickness ≈100 nm, the magnitude of the magnetic moment per Cr is estimated to be 0.028μB, too small to attribute to fully ferromagnetically-aligned localized Cr^{4+} ions (2 μB/Cr). Instead, similar to the case of $CaCrO_3$, it seems reasonable to attribute such weak ferromagnetism to a canted

antiferromagnetic spin structure.[10,20] The rotational distortion of the CrO_6 octahedra that likely causes the measured tetragonal phase in this sample also allows for a Dzyaloshinsky-Moriya (DM)[21,22] interaction, similar to the case for the canted Cu^{2+} moments in La_2CuO_4. Further measurements, such as muon spin rotation and neutron diffraction, are necessary before we reach a decisive conclusion on the magnetic structure.

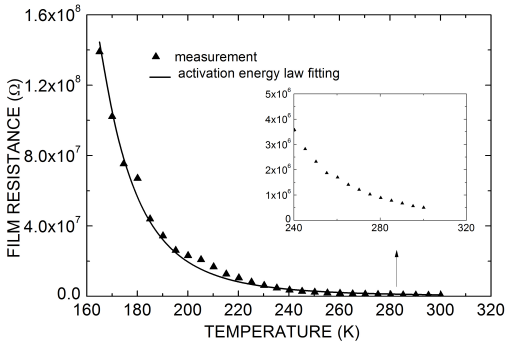

FIG. 5: Resistance versus temperature for the epitaxial $BaCrO_3$ thin film on a STO(001) substrate: closed triangles -measured values and solid line - fit to activation law yielding an energy parameter $\Delta \approx$ 0.38 eV.

Figure 5 shows the measured $BaCrO_3$ film resistance (closed triangles) as a function of temperature revealing that $BaCrO_3$ is insulating. The variation of the resistance with temperature can be fit with the activation law $\rho = \rho_0 \exp[-\Delta / (K_B T)]$ yielding $\Delta \approx 0.38$ eV, which is smaller than that previously reported for $PbCrO_3$ ($\approx$0.5 eV).[14] Among the chromate compounds reported to date, $PbCrO_3$ is an insulator in accordance with its significantly large lattice constant, while $SrCrO_3$ and $CaCrO_3$, both with smaller unit-cell volume, are controversial in that they have been reported to have behavior ranging from insulating to metallic. This has resulted in the conjecture that these two compounds are close to the crossover from the localized to itinerant electronic states. The ionic radii range from Ca^{2+} to Ba^{2+}: r(Ca^{2+}(VIII)) = 1.12Å, r(Sr^{2+}(VIII)) = 1.26Å, r(Pb^{2+}(VIII)) = 1.29Å, r(Ba^{2+}(VIII)) = 1.42Å.[23] Correspondingly, the pseudocubic lattice parameter of the compound also increases, ac(Ca) = 3.75Å, ac(Sr) = 3.82Å, ac(Pb) = 4.00Å, and ac(Ba) = 4.07Å. $BaCrO_3$ therefore exhibits the largest lattice parameter in this chromate family, much greater than previously predicted value 3.85Åby density functional theory (DFT) calculation.[24] Due to the fully-filled orbital configurations of Ca^{2+}, Sr^{2+}, and Ba^{2+}, the electronic structures of these chromate compounds are mainly determined by the corner-sharing CrO_6 octahedra. Therefore, one might think that the electronic phases of these chromate compounds, ranging from metallic to insulating, could be understood in a unified scheme, namely, a variation of the ionic radius modifies the octahedral unit cell, resulting in a Mott transition. However, the Mott transition is expected to be accompanied by a nonmagnetic to antiferromagnetic transition while similar materials, such as manganites, undergo a ferromagnetic to antiferromagnetic transition. In this case, the magnetism appears mostly unaffected by the conductivity change of the samples; an unexpected result.

In conclusion, we report the epitaxial growth of a $BaCrO_3$ film with the perovskite structure, which to date has not been obtained in the powder samples made by standard solid-state synthesis techniques. This material, exhibiting weak ferromagnetism which is possibly due to a canted antiferromagnetic spin structure, has much in common with other chromate family members and should serve as an important example for understanding the magnetic structure of the TMOs. It will also be of interest to see if the $BaCrO_3$ film can be made metallic by choosing appropriate substrates and modifying the thickness of the films, which will help to clarify the controversial reports concerning the transition properties of bulk $CaCrO_3$ and $SrCrO_3$.

We thank L. Narangammana, H. E. Mohottala, and Y. F. Nie for helpful discussions. This work is supported by the NSF through grants DMR-0907197.

[1] M. Imada, A. Fujimori, and Y. Tokura, Rev. Mod. Phys. 70, 1039-1263 (1998).
[2] P. Schiffer, A. P. Ramirez, W. Bao, and S.-W. Cheong, Phys. Rev. Lett. 75, 3336 (1995).
[3] D. I. Khomskii and G. A. Sawatzky, Solid State Commun. 102, 87 (1997).
[4] Y. Yoshida, S. I. Ikeda, H. Matsuhata, N. Shirakawa, C. H. Lee and S. Katano, Phys. Rev. B 72, 054412 (2005).
[5] B. L. Chamberland and C. W. Moeller, J. Solid State Chem. 5, 39 (1972).
[6] B. L. Chamberland and C. W. Moeller, Solid State Commun. 5, 663 (1967).
[7] J. B. Goodenough, J. M. Long, and J. A. Kafalas, Mater. Res. Bull. 3, 471 (1968).
[8] J. F. Weiher, B. L. Chamberland, and J. L. Gillson, J. Solid State Chem. 5, 39 (1972).
[9] W. L. Roth and R. C. DeVires, J. Appl. Phys. 38, 951 (1967).
[10] J. S. Zhou, C. -Q. Jin, Y. -W. Long, L. -X.Yang, and J. B. Goodenough, Phys. Rev. Lett. 96, 046408 (2006).
[11] A. J. Williams, A. Gillies, and J. P. Attfield, G. Heymann, H. Hupertz, M. J. Martinze-Lope, and J. A. Alonso, Phys. Rev. B 73, 104409 (2006).
[12] L. Ortega-San-Martin, A. J. Williams, J. Rodgers, J. P. Attfield, G. Heymann, and H. Huppertz, Phys. Rev. Lett. 99, 255701 (2007).
[13] A. C. Komarek, S. V. Streltsov, M. Isobe, T. Moller, M. Hoelzel, A. Senyshyn, D. Trots, M. T. Fernandez-Diaz, T. Hansen, H. Gotou, T. Yagi, Y. Ueda, V. I. Anisimov, M. Gruninger, D. I. Khomskii, and M. Braden, Phys.

Rev. Lett. 101, 167204 (2008).
[14] S. V. Streltsov, M. A. Korotin, V. I. Anisimov, and D. I. Khomskii, Phys. Rev. B 78, 054425 (2008).
[15] A. C. Komarek, T. Moller, M. Isobe, Y. Drees, H. Ulbrich, M. Azuma, M. T. Fernandez-Diaz, A. Senyshn, M. Hoelzel, G. Andre, Y. Ueda, M. Gruninger, and M. Braden, Phys. Rev. B 84, 125114 (2011).
[16] P. A. Bhobe, A. Chainani, M. Taguchi, R. Eguchi, M. Matsunami, T. Ohtsuki, K. Ishizaka, M. Okawa, M. Oura, Y. Senba, H. Ohashi, M. Isobe, Y. Ueda, and S.Shin, Phys. Rev. B 83, 165132 (2011).
[17] B. L. Chamberland, J. Solid State Chem. 43, 3 (1982).
[18] P. S. Haradem, B. L. Chamberland, L. Katz, J. Solid State Chem. 1, 34 (1979).
[19] C. -Q. Jin, J. S. Zhou, J. B. Goodenough, Q. Q. Liu, J. G. Zhao, L. X. Yang, Y. Yu, R. C. Yu, T. Katsura, A. Shatskiy, and E. Ito, Proc. Natl. Acad. Sci. USA, 105,7115 (2008).
[20] O. Ofer, J. Sugiyama, M. Mansson, K. H. Chow, E. J. Ansaldo, J. H. Brewer, M. Isobe, and Y. Ueda, Phys. Rev. B 184405 (2010).
[21] I. Dzyaloshinsky, J. Phys. Chem. Solids 4, 241 (1958).
[22] T. Moriya, Phys. Rev. 120, 91 (1960).
[23] R. D. Shannon, Acta Crystalloger. Sect. A 32, 751 (1976).
[24] Z. H. Zhu and X. H. Yan, J. Appl. Phys. 106, 023713 (2009).